A STUDY OF IN-REACTOR DENSIFICATION OF UO_2 FUEL IN THE MH-1A REACTOR

V. W. Storhok

Battelle Columbus Laboratories

Prepared for:

Army Facilities Engineering Support Agency
Atomic Energy Commission

23 December 1974

FINAL REPORT

on

A STUDY OF IN-REACTOR DENSIFICATION OF UO_2 FUEL IN THE MH-1A REACTOR

to

U.S. Army Facilities Engineering
Support Agency (FESA)

December 23, 1974

by

V. W. Storhok

BATTELLE
Columbus Laboratories
505 King Avenue
Columbus, Ohio 43201

TABLE OF CONTENTS

A STUDY OF IN-REACTOR DENSIFICATION OF UO_2 FUEL IN THE MH-1A REACTOR

by

V. W. Storhok

ABSTRACT

Density data obtained by a mercury pycnometry technique provided conclusive evidence that the UO_2 fuel in the MH-1A Reactor densified during operation. On the basis of optical metallographic observations, the densification occurred by annihilation of small as-fabrication porosity. The fuel densification did not result in any obvious decrease in the integrity of the fuel rods or the fuel assembly.

INTRODUCTION

A program to examine fuel rods from a spent MH-1A fuel assembly was conducted at the Battelle-Columbus Hot Laboratory Facility. The program was conducted for the U.S. Army Facilities Engineering Support Agency under USAEC Contract W-7405-eng-92. The primary objectives of the program were to:

(1) Determine the extent, if any, of UO_2 fuel densification that may have occurred during operation.

(2) Assess any effects fuel densification may have had on the integrity of the fuel rods and the assembly.

This study was prompted by problems encountered because of in-reactor densification of UO_2 fuel in Zircaloy-clad light water reactor fuel rods. The densification of UO_2 fuel during operation was resulted in shortening of fuel columns with attendant gap formation. Because of loss of support of the underlying fuel, collapse of the Zircaloy clad in the gap areas has occurred. In contrast to most current commercial light water reactor fuels, the MH-1A fuel columns are short (36 in.) and the cladding is stainless steel.

The study of MH-1A Reactor fuel densification involved the receipt of one spent fuel assembly, the nondestructive examination of six fuel rods removed from the assembly and the destructive examination of samples from two of the removed fuel rods. The nondestructive examinations consisted of visual examination, neutron radiography, gamma scanning, and fission gas sampling and analysis. Destructive examinations consisted of fuel burnup analysis, fuel density measurements and fuel metallographic examination.

DESCRIPTION OF MH-1A FUEL ASSEMBLY

MH-1A Type I Fuel Assembly No. 46 provided the fuel rods for study in this program. The Type I assemblies contain 104 stainless steel clad fuel rods arranged as shown in Figure 1. Plates at the top and bottom of the assembly position the fuel rods. The UO_2 fuel in each rod is in the form of pellets 1.0 in. long by 0.456 in. diameter stacked to a height of 36 in. Specifications called for an as-fabricated fuel density of 10.2 to 10.5 g/cc. The Type 348 stainless steel cladding has an ID of 0.461 in. and an OD of 0.507 in. A one-in.-long gas plenum is at the top of each fuel rod.

EXPERIMENTAL PROCEDURES AND RESULTS

The experimental procedures and results of the examinations are given in the following sections.

Visual Examination of Assembly

The fuel assembly was visually examined to assess its general condition. This examination showed the assembly to be in good condition with no evidence of extensive rod bowing, clad collapse, or any other type of damage. A photograph of one side of the assembly is shown in Figure 2.

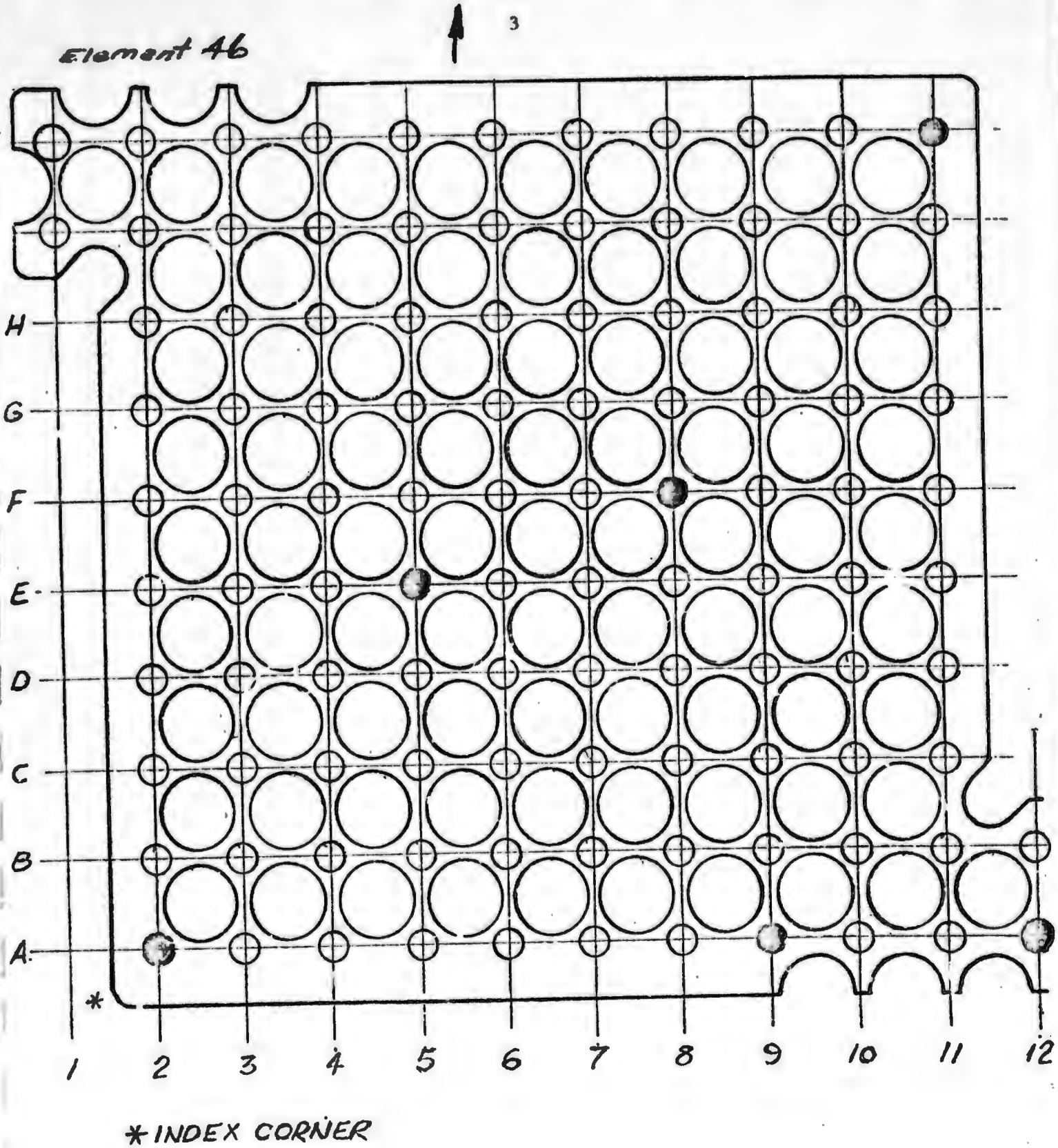

FIGURE 1. SKETCH OF TOP PLATE SHOWING LOCATIONS WHERE FUEL RODS WERE REMOVED FROM MH-1A ASSEMBLY No. 46

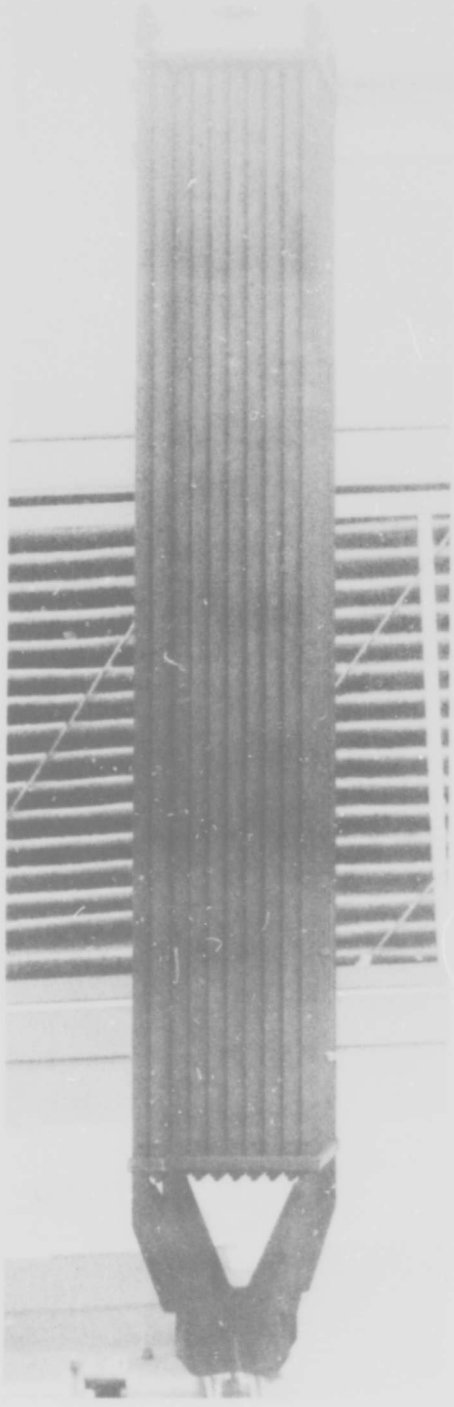

C1406

FIGURE 2. VIEW OF AS-RECEIVED MH-1A FUEL ASSEMBLY NO. 46 THROUGH HOT CELL WINDOW. The assembly appears sound in all respects.

Fuel Rod Removal

Six rods, A-2, A-9, A-12, E-5, F-8, and J-11 were removed from the assembly for detailed examination. Rod locations are shown in the sketch of the top grid plate, Figure 1. Corner rods, A-2, A-12, and J-11 were removed from the assembly by cutting through the top and bottom end caps with an abrasive wheel. To minimize chances of violating the rod containment, the end cap cuts were made as close as possible to the top and bottom grid plates. The inner rods A-9, E-5, and F-8 were removed by cutting 0.625 in. diameter holes through the grid plates and pulling the rods through the holes. The holes were cut with a drill saw.

Two 0.5 in. diameter stainless steel rods were inserted into the E-5 and F-8 positions and the assembly returned to the MH-1A Shipping Cask and shipped to Savannah River Labs for reprocessing.

Visual Examination of Fuel Rods

Each of the six removed fuel rods were examined visually using a stereoviewer. No evidence of clad collapse, distortion, or excessive corrosion was observed. Figures 3 and 4 show the highest performance region of Rods A-2 and A-9. As can be seen the cladding appears to be completely sound. The oxide coating on the rods was typical of that formed on stainless steel on exposure to high-temperature water. Figure 5 shows the bottom region of Rod E-5 where neutron radiography revealed an absence of fuel. If the fuel was missing during operation, it had no obvious deleterious effect on the cladding.

Neutron Radiography

All six removed rods were neutron radiographed with the objective of assessing gap formation in the fuel column and general fuel condition. Each rod was radiographed over its entire length in two orientations 90 degrees apart. Radiography was performed at the Battelle Research Reactor.

4X C1711

FIGURE 3. VIEW OF HIGH PERFORMANCE REGION OF ROD A-2, (HIGHEST BURNUP ROD EXAMINED) 8-1/2 - 9-1/2 IN. ABOVE THE BOTTOM OF THE FUEL COLUMN

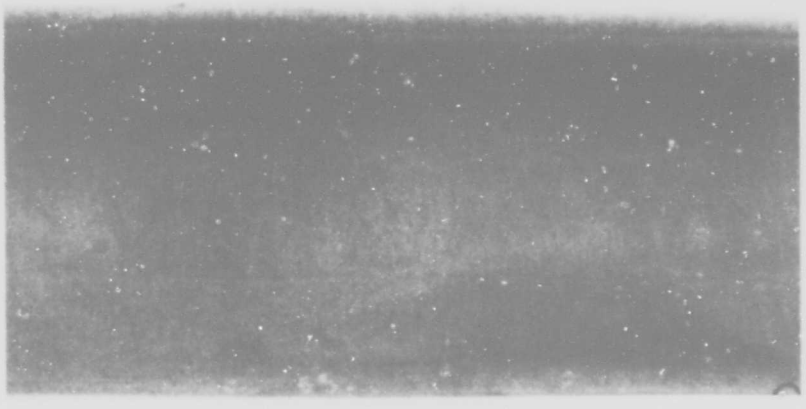

4X C1731

FIGURE 4. VIEW OF HIGH PERFORMANCE REGION OF ROD A-9 (SECOND HIGHEST BURNUP ROD EXAMINED), 17-1/2 - 18-1/2 IN. ABOVE THE BOTTOM OF THE FUEL COLUMN

4X C1711

FIGURE 3. VIEW OF HIGH PERFORMANCE REGION OF ROD A-2, (HIGHEST BURNUP ROD EXAMINED) 8-1/2 - 9-1/2 IN. ABOVE THE BOTTOM OF THE FUEL COLUMN

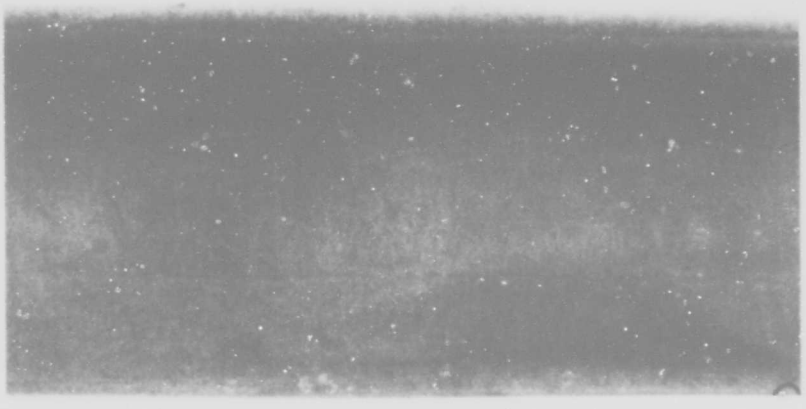

4X C1731

FIGURE 4. VIEW OF HIGH PERFORMANCE REGION OF ROD A-9 (SECOND HIGHEST BURNUP ROD EXAMINED), 17-1/2 - 18-1/2 IN. ABOVE THE BOTTOM OF THE FUEL COLUMN

The neutron radiographs, Figure 6, did reveal gaps in the fuel columns. Also, cracking of fuel pellets appeared to be moderately severe. However, movement of fuel within the rod was observed upon moving the rod from one radial position to another, suggesting a loose fit of fuel in the cladding. This looseness was later observed during sectioning and metallographic examination. In light of this loose fit and the absence of a holddown spring, the gap formation could have been caused by movement of the fuel during transport and handling. Similarly, the freedom of pellet movement could allow fuel fragments to slip out of normal pellet positions and make the fuel cracking appear more severe than usual. As will be seen later in this report, metallographic examination showed that the degree of cracking was typical of that resulting from thermal stresses in UO_2 fuel.

It is uncertain whether the fuel column gaps occurred before, during, or after operation. If any of the gaps were present during operation, they did not lead to any clad collapse. The stainless steel cladding apparently was strong enough to resist the clad collapse observed in similar situations with Zircaloy clad rods. Evidence of high clad strength is provided by the loose fit of the fuel in the cladding. Zircaloy clad tends to creep down under the pressure of the reactor water and eventually contact the fuel, at least in spots. The loose fuel fit in the MH-1A fuel rods indicates that no significant creep down of the stainless steel clad occurred.

Gamma Scanning

The six fuel rods were gamma scanned to determine the relative axial burnup by measuring the gross gamma activity as a function of rod axial position.

Each rod was scanned by moving the vertically positioned rod at a constant rate of 2 in. per minute past a collimating slit-detector arrangement and continuously measuring and recording on a strip chart the gamma ray intensity from that part of the pin passing the collimator. All energies greater than 0.5 MeV were measured and recorded. The detector used was a sodium iodide crystal. Collimators and slits were adjusted to maintain a counting rate sufficiently low to avoid dead time losses.

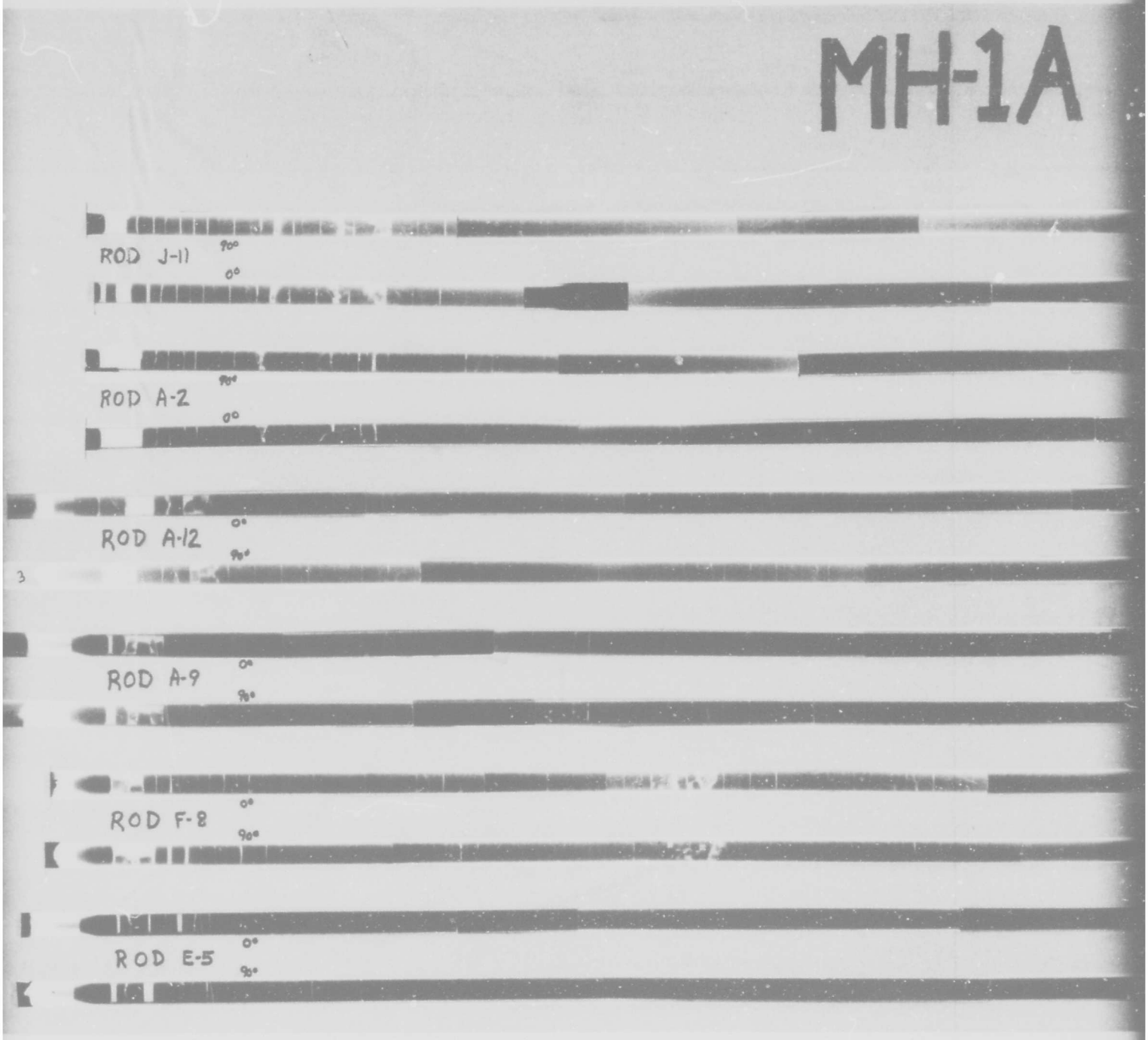

FIGURE 6. NEUTRON RADIOGRAPHS OF REMOVED MH-1A FUEL RODS. Note the cracked fuel
Also, note that some fuel moved within the rods when the rods were rota
(0 to 90 degrees). This movement is indicative of a very loose fit of

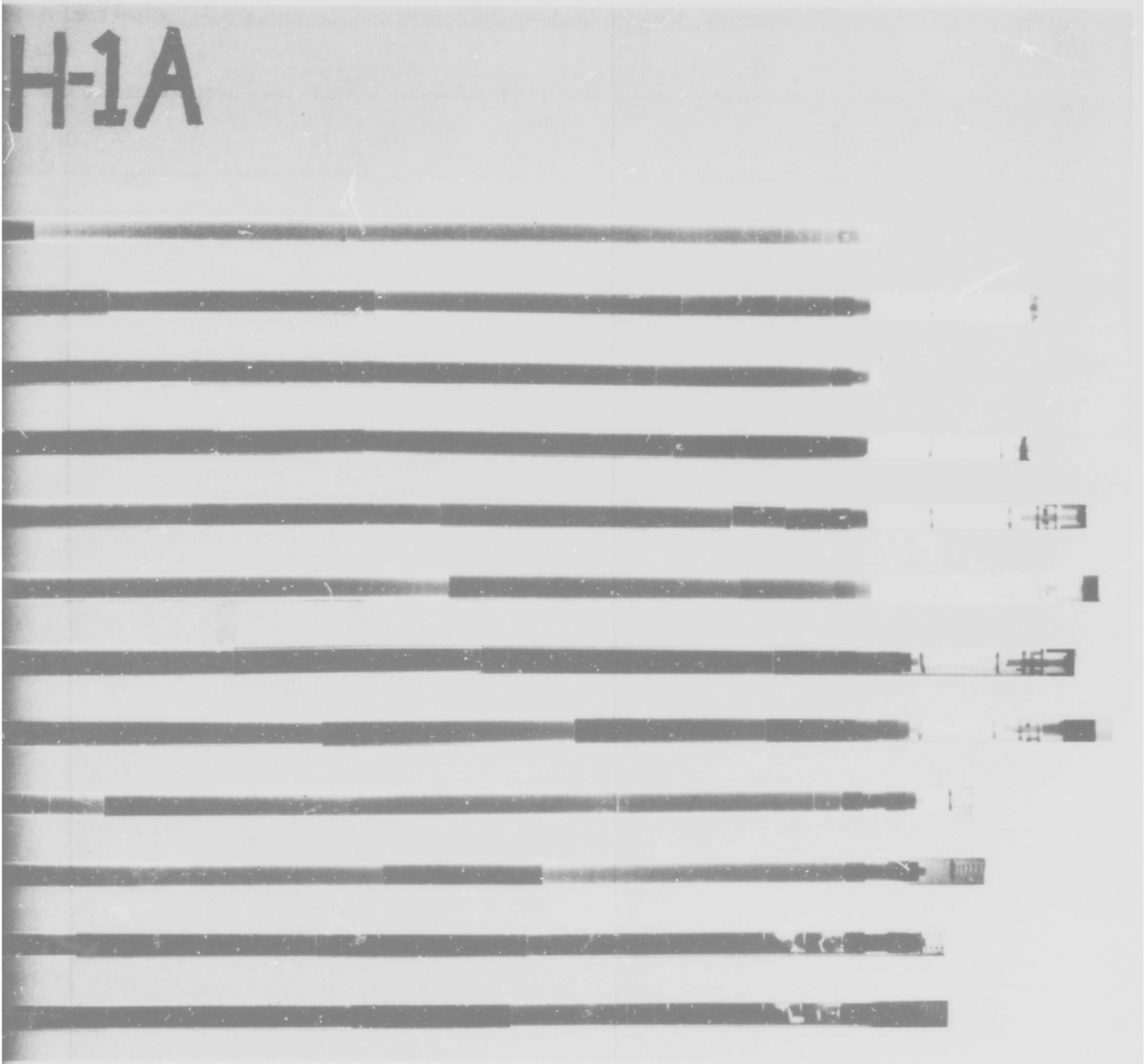

Note the cracked fuel and the gaps in some of the fuel columns. when the rods were rotated from one radial position to another of a very loose fit of fuel within the cladding.

The gamma scans, Figures 7 through 12 show that the peak activities occurred over a region from about 9 in. to 20 in. above the bottom of the fuel column. On the basis of the relative amplitudes of the gamma activities at peak burnup positions, Rod A-2 has experienced the highest burnup followed by Rod A-9 and Rod A-12. The activity levels of the other three rods are somewhat lower and approximately equal.

Localized dips in the gamma activity indicate gaps in some of the fuel columns, notably in Rods J-11, E-5, and A-9. In light of evidence that the fuel pellets fit very loosely in the cladding, it is possible that these gaps formed because of shifting of pellets during transit and handling rather than because of fuel densification.

The gamma scan of Rod A-2 revealed activity spikes, apparently at pellet interfaces, in the high performance region. This type of behavior is usually attributed to migration of cesium to the pellet interfaces and is evidence of relatively high operating temperatures.

Fission Gas Analysis and Void Volume Measurements

The fission gases from the plenums of Rods A-2, A-9, E-5, F-8, and J-11 were collected for analysis and rod gas pressures and void volumes were measured. Rod A-12 was not subject to gas sampling as it was damaged during an in-cell transfer. Collection for analysis was accomplished by fitting the rod plenum in an evacuable sleeve, evacuating the sleeve, puncturing the cladding in the plenum region to release the gas from the rod, and Toeppler pumping the gases to collection vials. The rod gas volumes were determined by expanding the gas to an evacuated system of known volume and observing the pressure rise. The rod void volume was determined by expanding known quantities of helium into the pin and observing the pressure change. System calibrations have shown that the gas volumes determined from these measurements are accurate to within ±3 percent.

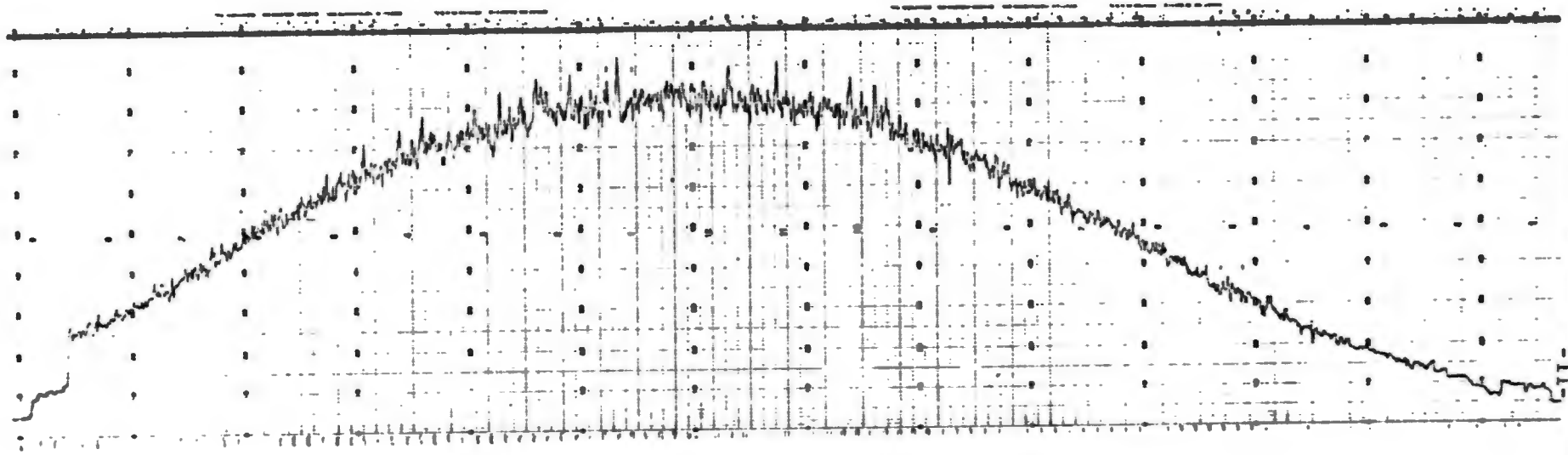

FIGURE 7. GAMMA SCAN OF RODS A-2. This is the highest burnup rod examined in this program. Note the activity spikes in the high performance region of the rod. Spikes of this type are generally attributed to migration of cesium to the pellet ends.

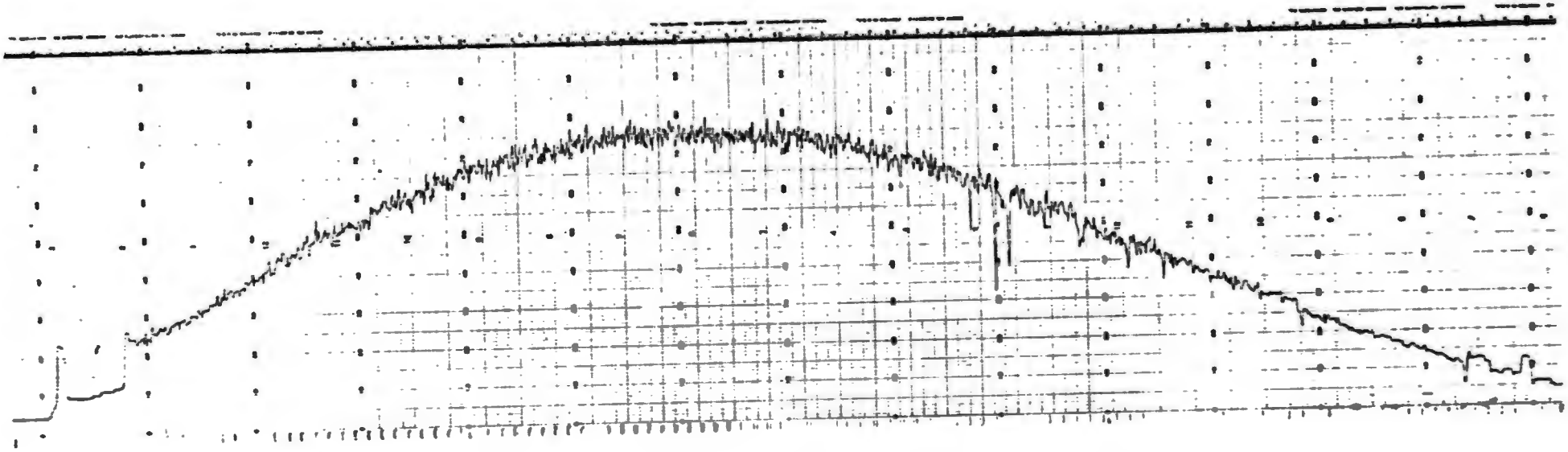

FIGURE 8. GAMMA SCAN OF ROD A-9. This is the second highest burnup rod examined. The dips in activity toward the top of the rod are indicative of gaps in the fuel column.

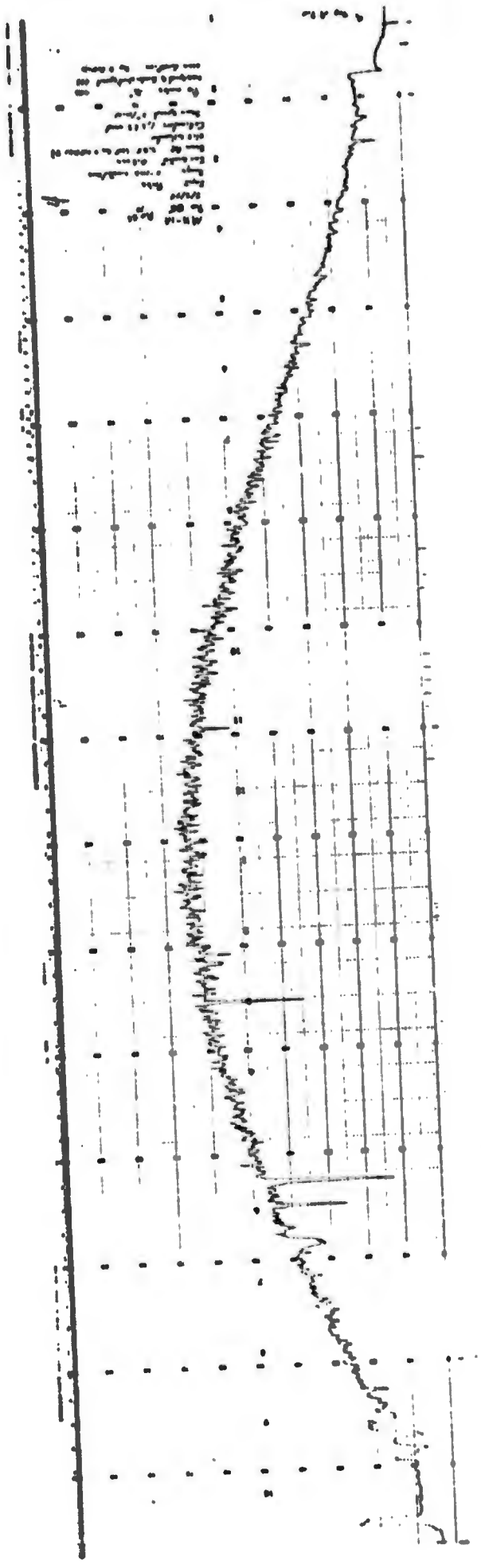

FIGURE 9. GAMMA SCAN OF ROD E-5. Sharp dips in activity are indicative of gaps in the fuel column.

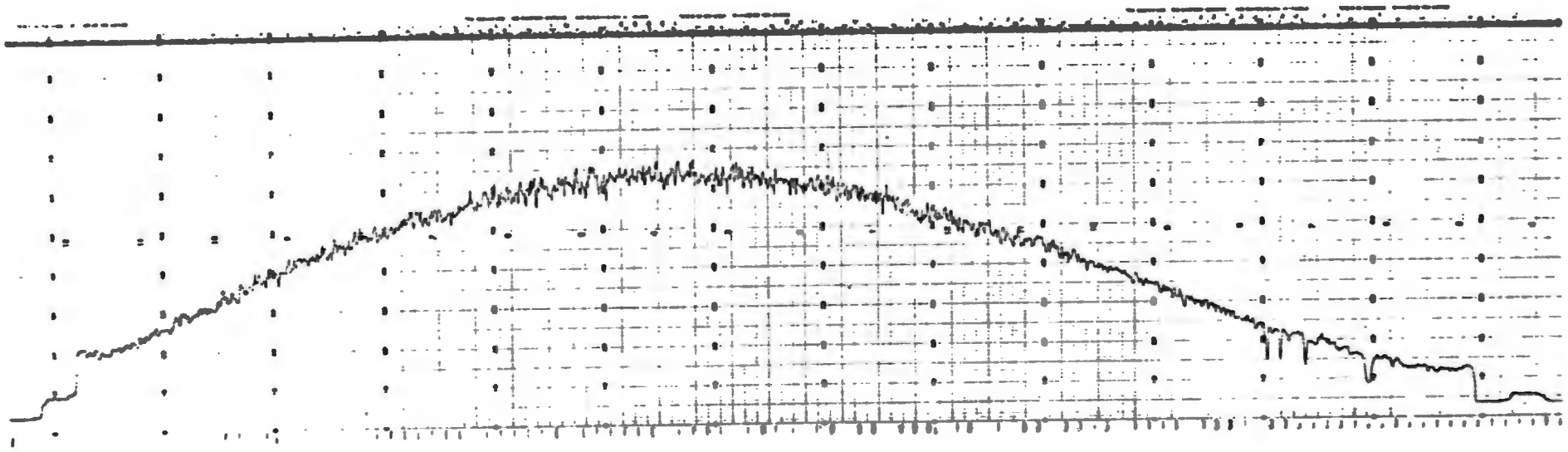

FIGURE 10. GAMMA SCAN OF ROD A-12. A few small gaps in the fuel column are evident near the top of the rod.

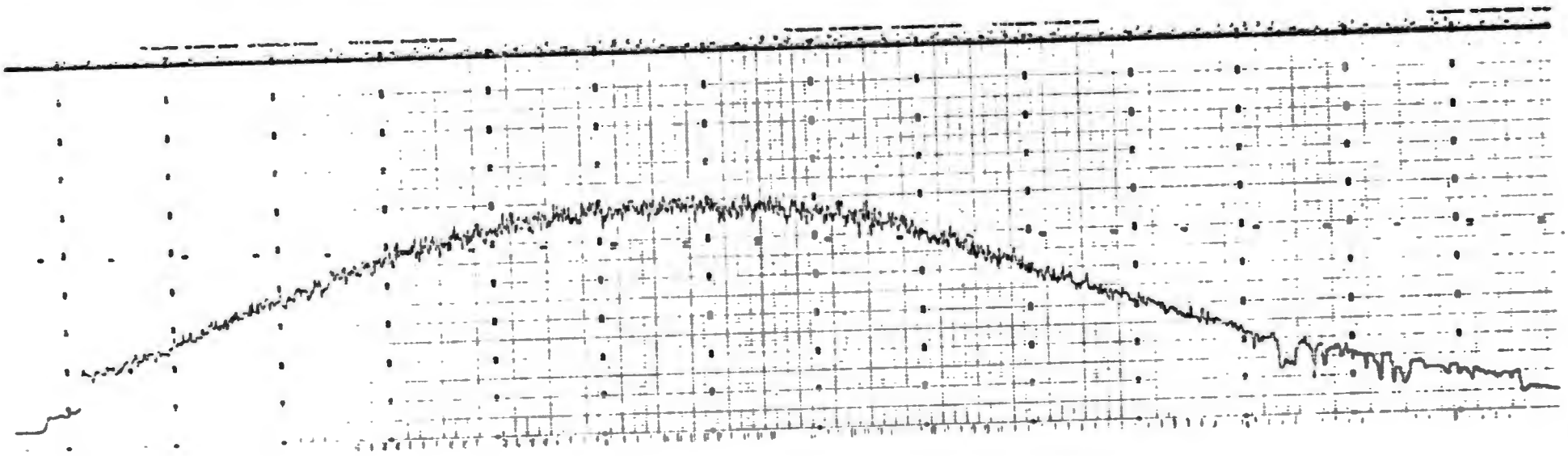

FIGURE 11. GAMMA SCAN OF ROD J-11. Dips near the top of the fuel column suggest gaps and possible fuel pellet fragmentation.

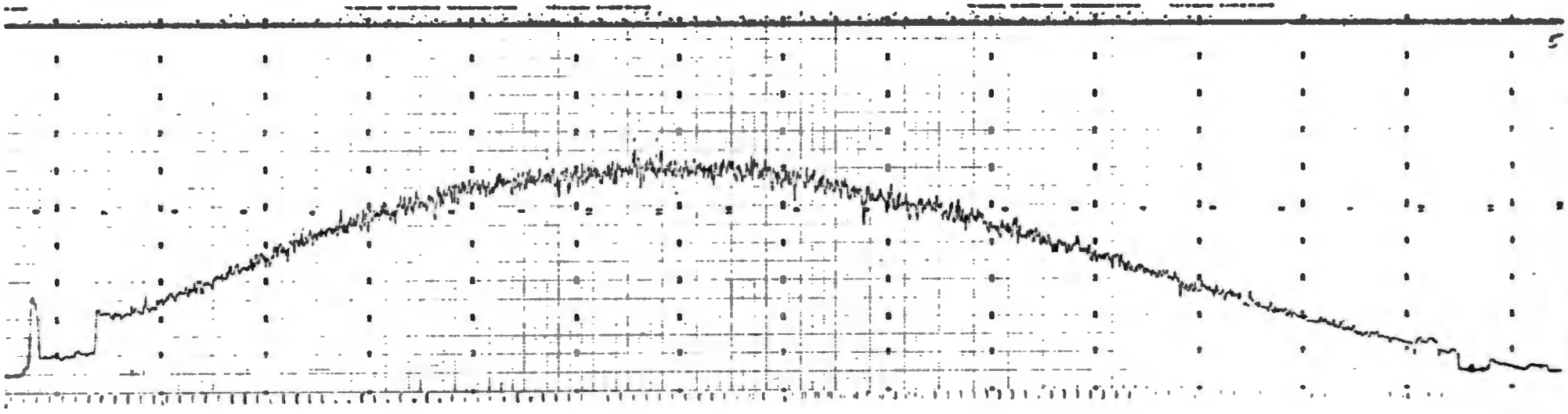

FIGURE 12. GAMMA SCAN OF ROD F-8. Fuel pellet column appears to be intact.

The collected gases were analyzed qualitatively and quantitatively using mass spectrometric techniques. Results of these measurements and analyses are given in Tables 1 and 2.

Fission gas releases were calculated on the basis of average fuel rod burnups as determined from burnup analysis and gamma scanning and a total fuel volume in each rod of 96.5 cc.

Fission gas releases from Rods A-9, E-5, F-8, and J-11 were low, on the order expected from recoil (0.1 to 0.2 percent). Fission gas release from Rod A-2 (highest burnup rod) was considerably higher (4.8 percent) suggesting that fuel operating temperatures were high enough to promote gas migration. This was later substantiated when metallographic examination of a fuel sample from the high performance region of Rod A-2 revealed grain growth and fission gas porosity on the grain boundaries in the fuel center.

It is also interesting that the end-of-life gas pressures (at 0°C) were less than atmospheric in all rods other than A-2. Apparently for some reason the helium cover gas pressure of one atmosphere was not attained during rod fabrication.

Sectioning

Two fuel rods, A-2 and F-8 were selected for destructive examinations consisting of fuel density measurements, metallography and burnup analysis. Sections for these studies were removed as shown in Table 3. Sample locations were selected to obtain samples over a broad range of burnup levels.

In light of the looseness of the fuel in the cladding, problems in loss of fuel from the cut sections were anticipated. For this reason, sectioning was accomplished using a tubing cutter. It was felt that the crimped edges of the tubing cut would tend to hold the fuel in place. The alternate sectioning technique would have been by an abrasive cutting wheel. Vibrations from the cutting wheel would probably have tended to shake out the fuel. Insofar as possible, the cuts were made at pellet interfaces as determined from neutron radiographs.

TABLE 1. RESULTS OF MASS SPECTROMETRIC ANALYSES OF GASES FROM MH-1A FUEL RODS

Rod No.	Total Gas Quantity, cc at STP	Volume Percent										Fission Gas Release, Percent
		H_2	Hlie	CH_4	H_2O	O_2	N_2	AAr	CO_2	Kr	Xe	
A-2	22.69	<0.01	29.7	<0.01	<0.1	<0.01	0.22	0.03	<0.01	9.49	60.60	4.8
A-9	5.58	<0.01	90.2	<0.01	<0.1	0.67	3.18	0.05	<0.05	0.80	5.10	5.10
E-5	9.39	<0.01	87.3	0.01	0.7	0.01	1.29	0.12	<0.1	0.95	9.07	0.2
F-8	9.85	<0.01	90.6	<0.01	<0.1	<0.01	0.21	0.03	<0.05	1.30	7.86	0.2
J-11	5.98	<0.01	86.7	<0.01	<0.1	0.43	3.67	0.07	<0.01	1.31	7.84	0.2

Rod No.	Kryton and Xenon Isotopic Ratios							
	^{83}Kr	^{84}Kr	^{85}Kr	^{86}Kr	^{131}Xe	^{132}Xe	^{134}Xe	^{136}Xe
A-2	13.8	28.7	6.1	51.4	10.7	20.3	31.3	37.7
A-9	13.9	28.6	6.3	51.2	11.1	19.9	31.4	37.6
E-5	13.9	28.4	6.2	51.5	11.3	20.0	32.4	36.3
F-8	13.9	27.6	6.6	51.9	11.3	20.0	32.7	36.0
J-11	14.1	28.2	6.2	51.5	11.2	19.4	32.4	37.0

TABLE 2. RESULTS OF GAS SAMPLING AND VOID VOLUME MEASUREMENTS OF MH-1A FUEL RODS

Rod	Gas Volume, cc at STP	Void Volume in Rod, cc	EOL Pressure in Rod at 0°C, psi
A-2	22.69	7.81	42.71
E-5	6.56	7.72	12.49
F-8	6.85	6.86	14.67
J-11	5.98	8.07	10.89
A-9	5.58	7.33	11.20

TABLE 3. SECTIONS REMOVED FROM RODS A-2 AND F-8 FOR DESTRUCTIVE EXAMINATION

Rod	Location, in. from bottom of fuel column	Burnup MWD/MTU(a)	Sample Type
A-2	4-5/32 - 4-3/4	11,900	Density
A-2	4-3/4 - 5-11/32	12,700	Metallography
A-2	13-3/32 - 13-11/16	18,200	Density
A-2	13-11/16 - 14-9/32	18,200	Metallography
A-2	14-9/32 - 14-7/8	18,200	Burnup Analysis
A-2	28-5/32 - 28-3/4	8,600	Metallography
A-2	28-3/4 - 29-11/32	8,000	Density
F-8	4-3/16 - 4-13/16	9,400	Metallography
F-8	4-13/16 - 5-13/32	10,000	Density
F-8	13-25/32 - 14-3/8	14,700	Metallography
F-8	14-3/8 - 15	14,700	Density
F-8	15 - 15-19/32	14,700	Burnup analysis
F-8	31-7/8 - 32-1/2	5,700	Burnup analysis
F-8	32-1/2 - 33/18	5,400	Metallography
F-8	33-1/8 - 33-11/16	4,800	Density

(a) Determined subsequent to sectioning from burnup analysis and gamma scan data.

Although some pieces of fuel were lost, the tubing cutter sectioning techniques worked quite well, and satisfactory samples were obtained for the destructive examinations.

Fuel Burnup Analysis

The absolute burnups of three fuel samples (one from Rod A-2 and two from Rod F-8) were determined by ASTM Method E-321.

The samples were dissolved by refluxing in 12N nitric acid. The dissolved samples were diluted with 4N nitric acid to a concentration of uranium of 0.001 g/cc. Only new glassware cleaned in boiling 8N nitric acid (ASTM Procedure E-267) was used for the dissolution. Aliquots of the solutions were sent to a mass spectrometer laboratory for heavy element isotopic and neodymium-148 analysis.

The resultant data were used to calculate burnup using the formula:

$$F_t = \frac{F'}{(U' + Pu' + F')} \times 100$$

where F_t = total heavy element atom percent fission

U' = total U atoms per sample

Pu' = total Pu atoms per sample

F' = number of fissions per sample (based on a fission yield of 1.68% for Nd-148)

Burnup in megawatt days per metric ton of uranium was calculated using the relationship MWD/MTU = Ft x 9600.

Rod	Sample location, in. from bottom of fuel column	Burnup, MWD/MTU
A-2	14-9/32 - 14-7/8	18,200
F-8	15 - 15-19/32	14,700
F-8	31-7/8 - 32-1/2	5,700

These data were used with the gamma scan data to estimate the burnups of the density and metallographic samples studied in this program. These estimated burnups are presented in the sections on metallography and density measurements. In addition, the burnup data were used to estimate average and maximum burnups of the six rods studied in this program. These data are shown below.

Rod	Burnup, MWD/MTU	
	Maximum	Average
A-2	18,200	12,600
A-9	17,200	12,200
A-12	15,000	10,500
E-5	15,000	10,400
F-8	14,700	10,200
J-11	14,000	10,000

Fuel Density Measurements

The objective of the density measurements was to quantitatively determine the bulk density of the UO_2 fuel at various levels of burnup. A mercury pycnometry technique was used for the density measurements. In this technique the sample weight is determined by direct weighing on an analytical balance. The sample volume is determined by measuring the volume of mercury displaced by the sample. This is accomplished by making a series of weight measurements of the pycnometer with and without the sample in the chamber. Volume is calculated by dividing displaced mercury weight by the handbook value for mercury density at the temperature of measurement. Mercury temperature is measured to with ±0.1°C at the time of measurement.

The technique is particularly applicable to bulk density measurements of porous materials as the mercury does not penetrate pores smaller than about 6 microns in diameter. This technique has a demonstrated precision and accuracy of ±0.2 percent as determined by measurement of a stainless steel standard with a known density of 7.908 g/cc.

As part of the system check, the density of the stainless steel standard was measured twice during the course of the fuel sample measurements. The results of the standard measurements are given along with the fuel density data in Table 4.

The fuel density data show that five out of six fuel samples had densities beyond the specified maximum as-fabricated fuel density (10.5 g/cc). This is regarded as conclusive evidence that the fuel densified during irradiation.

Because of the broad range of specified as-fabricated densities (10.2 to 10.5 g/cc) it is difficult to make any solid quantitative conclusions regarding the densification. On a conservative basis, assuming a starting density of 10.5 g/cc it can be stated that the maximum measured fuel density of 10.650 g/cc represents a 1.5 percent density increase. In a more speculative vein, a plot of density versus burnup, Figure 13, suggests that densification continued to a burnup of about 8000 MWD/MTU. The fuel then started to swell at a low rate as burnup continued. If it could be established that all of the fuel started life at approximately the same density, the validity of conclusions drawn from this plot would be strengthened. Behavior of this type would be expected, however. Early in life, when fission product inventory is low, densification should be the dominant process. Later, as the fuel approaches its maximum attainable density and as fission products buildup, the fuel should start to swell.

Metallographic Examination

The objectives of the metallographic examination were to qualitatively characterize the changes in pore size distribution and grain size as a result of irradiation to various levels of burnup.

TABLE 4. RESULTS OF FUEL DENSITY MEASUREMENTS

Rod	Location, in. from bottom of fuel column	Burnup, MWD/MTU	Density, g/cc
Stainless Steel Std	---	---	7.906
A-2	4-5/32 - 4-3/4	11,900	10.628
A-2	13-3/32 - 13-11/16	18,200	10.582
A-2	28-3/4 - 29-11/32	8,000	10.650
F-8	4-13/16 - 5-13/32	16,000	10.537
F-8	14-3/8 - 15	14,700	10.622
F-8	33-1/8 - 33-11/16	4,800	10.484
Stainless Steel Std	---	---	7.911

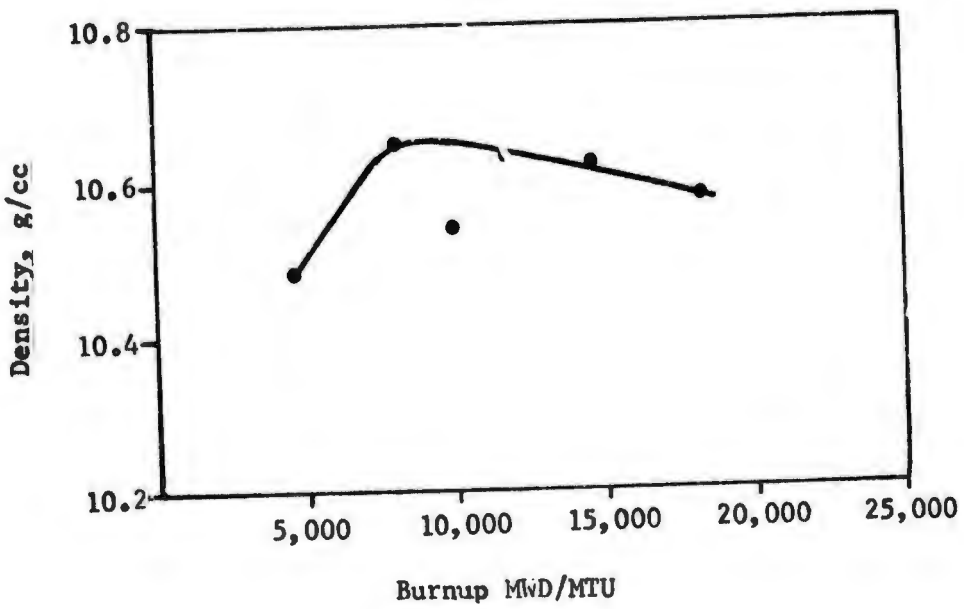

FIGURE 13. PLOT OF DENSITY VERSUS BURNUP.
This plot suggests that density increases with burnup with additional burnup, the fuel starts to swell at a low rate.

To meet these objectives the following six samples were examined metallographically:

Rod	Sample Location, in. from bottom of fuel column	Burnup, MWD/MTU
A-2	4-3/4 - 5-11/32	12,700
A-2	13-11/16 - 14-9/32	18,200
A-2	28-5/32 - 28-3/4	8,600
F-8	4-3/16 - 4-13/16	9,400
F-8	13-25/32 - 14-3/8	14,700
F-8	32-1/2 - 33-1/8	5,400

Sample preparation consisted of mounting the sample in epoxy, grinding through 600 grid SiC and polishing with Linde A-chromic acid on Texmet cloth. Etching to bring out UO_2 grains was accomplished by swabbing with a solution of 15 parts H_2SO_4-85 parts H_2O_2.

Each specimen was treated identically and the following photographs taken.

(1) 3.5X macroview of the as-polished specimens

(2) 100X radial fuel traverse, as-polished and etched

(3) 500X photographs as fuel center, mid radius, and surface, as-polished and etched

For this report, all of the macroviews are shown to illustrate cracking patterns. The 500X as-polished photographs are shown to illustrate changes in pore distribution at various levels of burnup. Only the highest and second highest burnup 100X radial traverses and 500X etched structures are shown to illustrate grain growth in the highest burnup sample and the absence of grain growth in the second highest burnup samples.

The macroviews, Figure 14, show the usual cracking patterns that result from thermal stress in the UO_2. Some loss of fuel has been experienced but this can be attributed to the loose fit of fuel in the cladding.

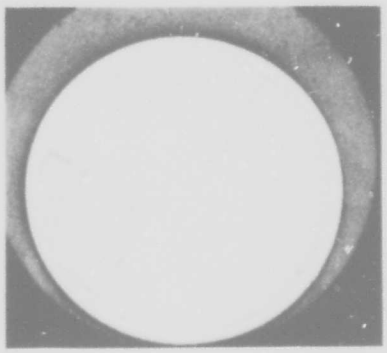

3.5X HC39441
(a) F-8.32-1/2 - 33-1/8 in.

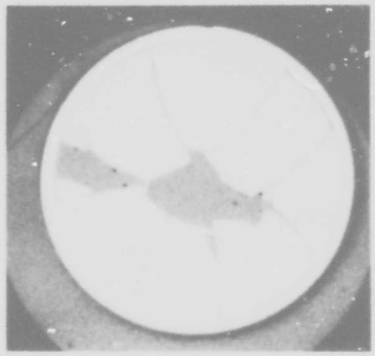

3.5X HC39442
(b) A-2. 28-5/32 - 28-3/4 in.

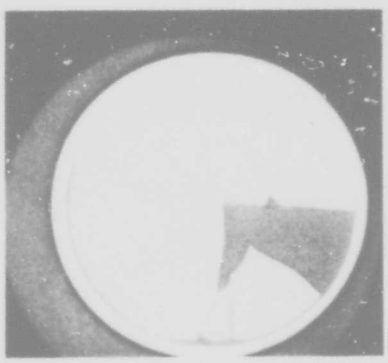

3.5X HC39439
(c) F-8. 4-3/16 - 4-13/16 in.

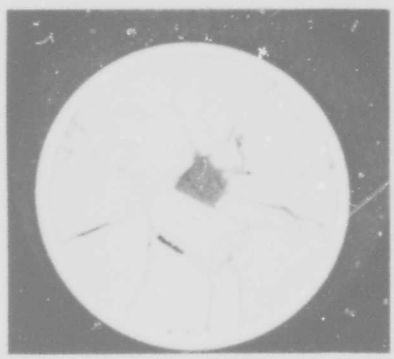

3.5X HC39444
(d) A-2. 4-3/4 - 5-11/32 in.

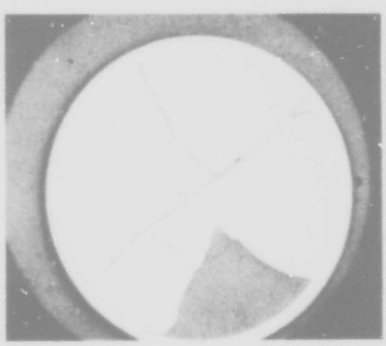

3.5X HC39440
(e) F-8. 13-25/32 - 14-3/8 in.

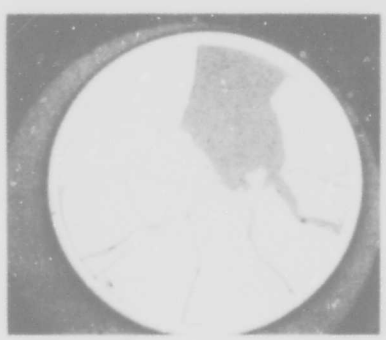

3.5X HC39443
(f) A-2. 13-11/16 - 14-7/32 in.

FIGURE 14. MACROVIEW OF METALLOGRAPHIC SPECIMENS. Cracking patterns are typical of these caused by thermal strusses in UO_2.

As-polished 500X photomicrographs of the fuel are presented in order of increasing burnup, Figures 15 through 20. Note that the lowest burnup sample contains a large number of small round pores plus a small number of large angular pores. With its low burnup, this sample probably best represents the as-fabricated pore structure. As burnup increases, the distribution of large pores stays about the same while the population of small pores decreases. Note that the high burnup specimens contain very few small pores. On the basis of these observations, it appears that densification occurred via annihilation of the small as-fabricated porosity. This same type of small pore annihilation has been observed in densified commercial reactor fuel.

Note that the center region of Specimen A-2 13-11/16 - 14-9/32 in. (highest burnup metallography sample) has enlarged grains and relatively large pores decorating the grain boundaries, Figures 21 and 22. This region of fuel operated at temperatures high enough to promote grain growth and fission gas migration. Recall that fission gas release from Rod A-2 was much higher than from the other rods. On the basis of the grain size, it appears that temperatures in the fuel center were on the order of 1300 to 140C C. Grain growth was not apparent in Rod F-8 at 13-25/32 - 14-3/8 in., Figures 23 and 24, or in any lower burnup samples, suggesting that the maximum operating temperatures in the other regions examined were less than 1000 or 1100 C.

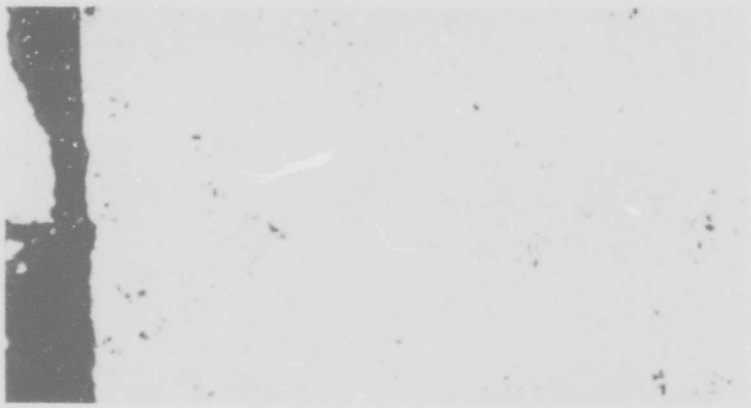

(a) Fuel Surface
500X
HC39664

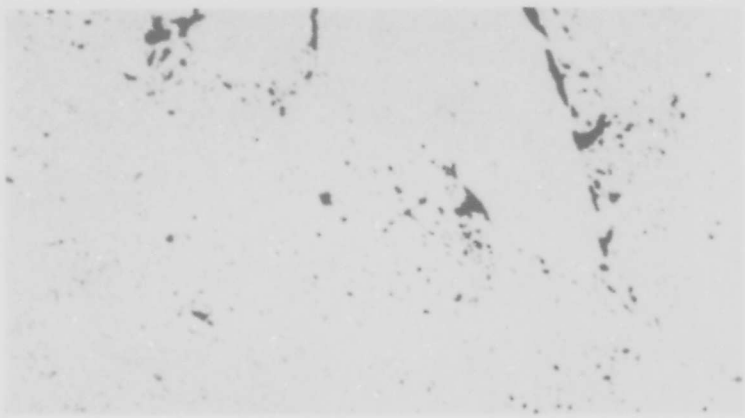

(b) Mid Radius
500X
HC39665

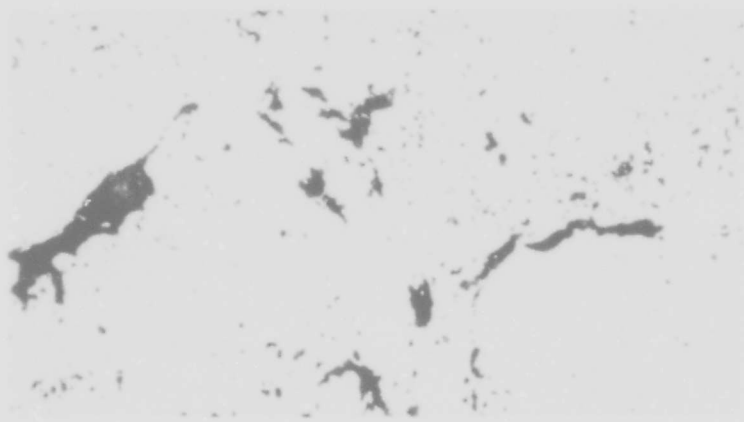

(c) Fuel Center
500X
HC39667

FIGURE 15. AS POLISHED MICROSTRUCTURE OF ROD F-8 AT 32-1/2 - 33-1/8 IN. FROM BOTTOM OF FUEL COLUMN. Burnup 5,400 MWD/MTU. Note the relative large population of small pores.

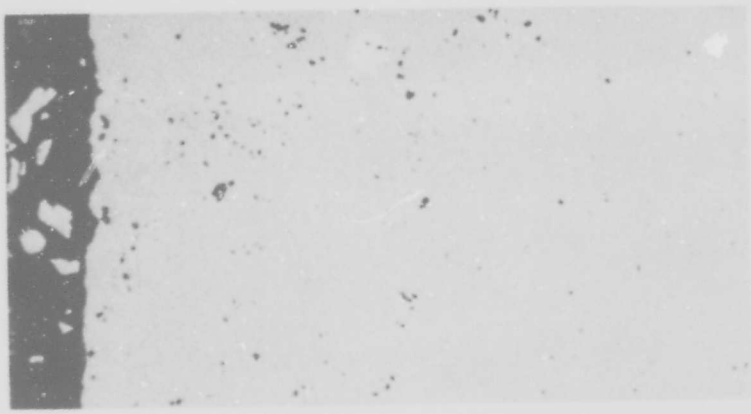

(a) Fuel Surface
500X
HC39668

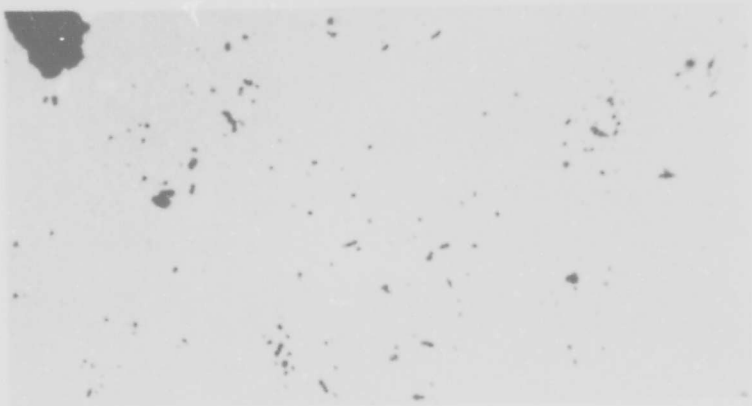

(b) Mid Radius
500X
HC39669

(c) Fuel Center
500X
HC39670

FIGURE 16. AS-POLISHED MICROSTRUCTIRE OF ROD A-2 AT 28-5/32 - 28-3/4 IN. FROM BOTTOM OF FUEL COLUMN. Burnup 8,600 MWD/MTU.

(a) Fuel Surface
500X
HC39660

(b) Mid Radius
500X
HC39661A

(c) Fuel Center
500X
HC39662A

FIGURE 17. AS-POLISHED MICROSTRUCTURE OF ROD F-8 AT 4-3/16 - 4-13/16 IN. FROM BOTTOM OF FUEL COLUMN. Burnup 9,400 MWD/MTU.

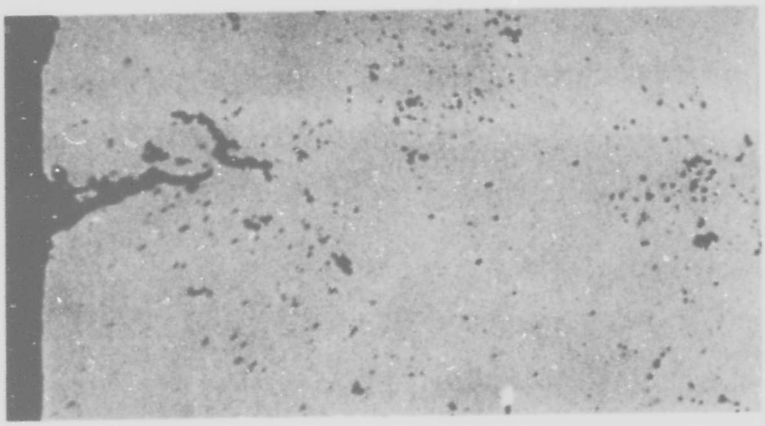

(a) Fuel Surface
500X
HC39676

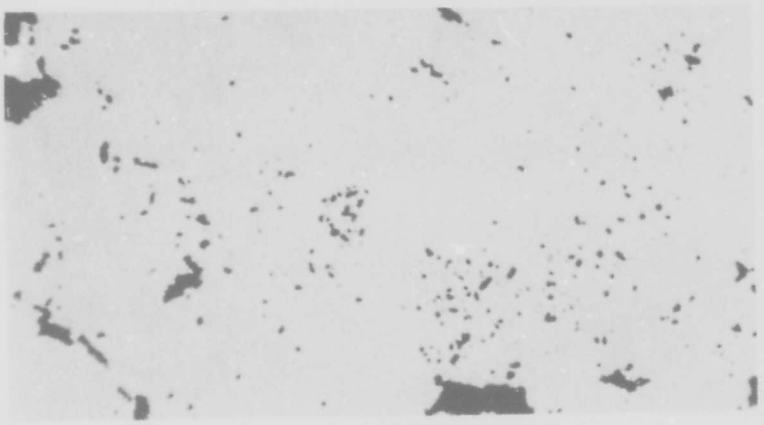

(b) Mid Radius
500X
HC39678

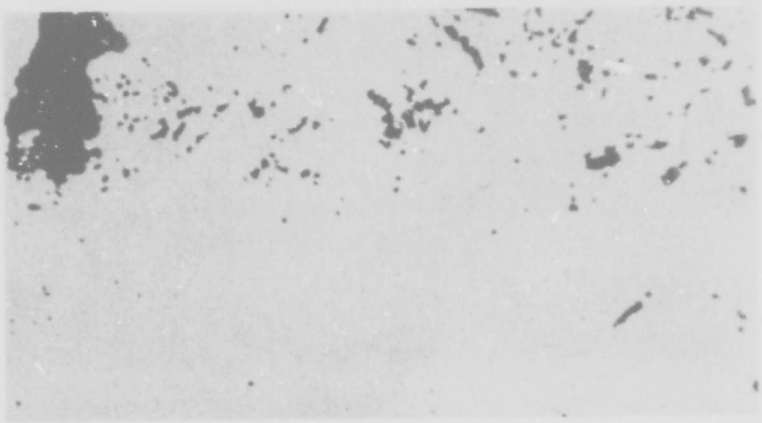

(c) Fuel Center
500X
HC39679

FIGURE 18. AS POLISHED MICROSTRUCTURE OF RCD A-2 at 4-3/4 to 5-11/32 IN. FROM BOTTOM OF FUEL COLUMN. Burnup 12,700 MWD/MTU.

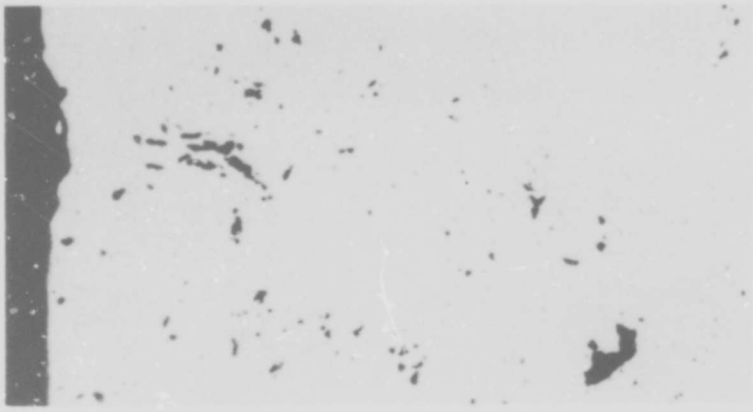

(a) Fuel Surface
500X
HC39661

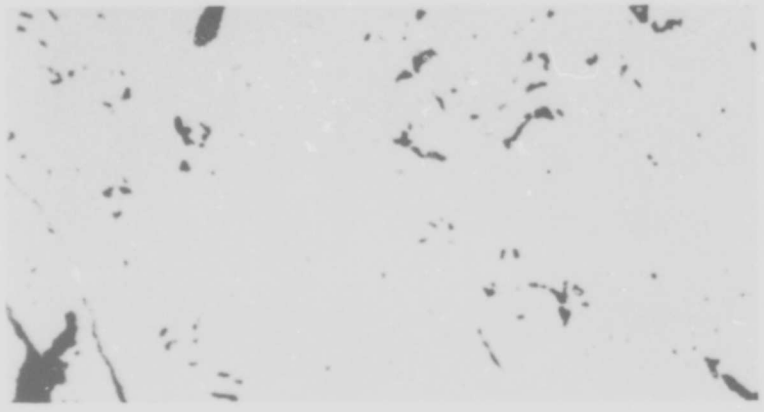

(b) Mid Radius
500X
HC39662

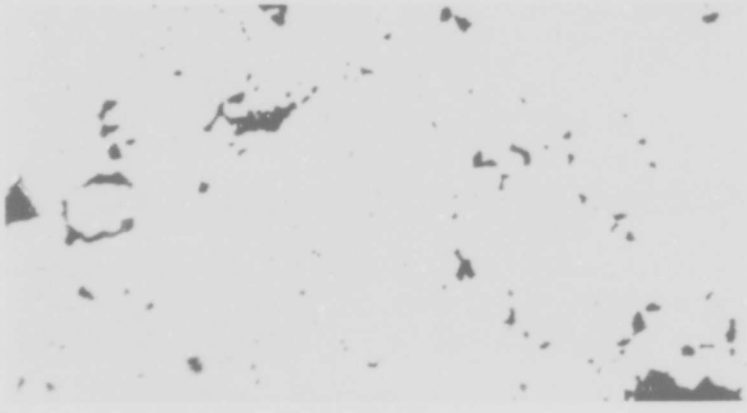

(c) Fuel Center
500X
HC39663

FIGURE 19. AS-POLISHED MICROSTRUCTURE OF ROD F-8 AT 13-25/32 - 14-3/8 IN. FROM BOTTOM OF FUEL COLUMN. Burnup 14,700 MWD/MTU.

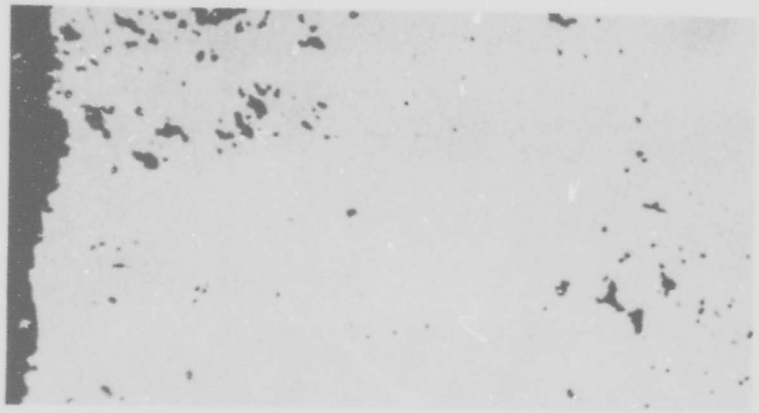

(a) Fuel Surface
500X
HC39671

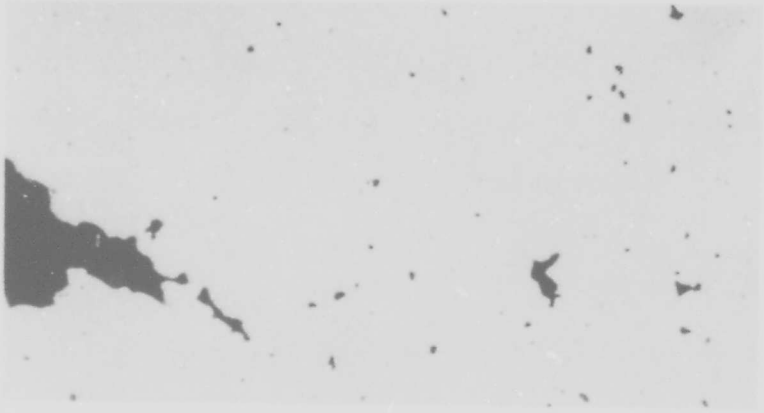

(b) Mid Radius
500X
HC39673

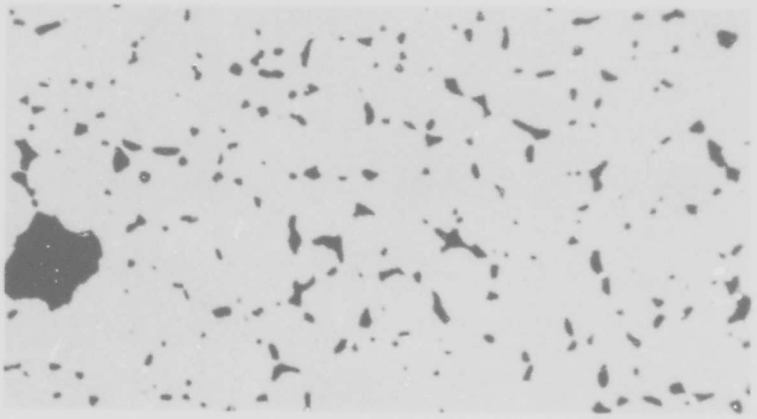

(c) Fuel Center
500X
HC39675

FIGURE 20. AS POLISHED MICROSTRUCTURE OF ROD A-2 AT 13-11/16 - 14-9/32 IN. FROM BOTTOM OF FUEL COLUMN. Burnup 18,200 MWD/MTU. Note the small population of small pores in the fuel surface and mid-radius positions. In fuel center, grains have grown and fission gas porosity decorates grain boundaries.

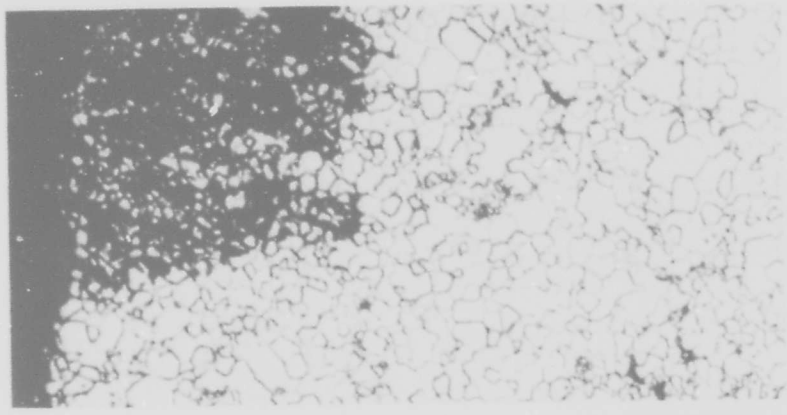

(a) Fuel Surface
500X
HC39727

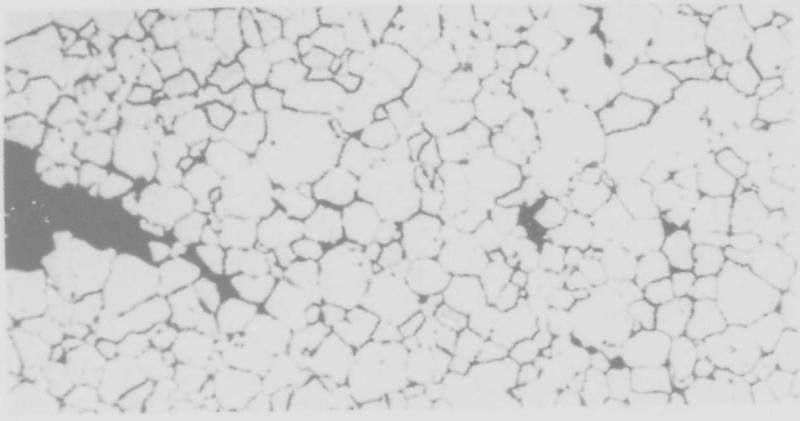

(b) Mid Radius
500X
HC39729

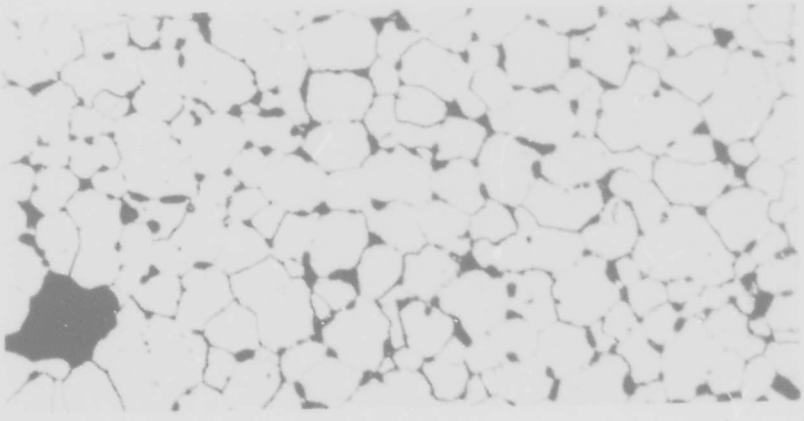

(c)Fuel Center
500X
HC39731

FIGURE 21. ETCHED MICROSTRUCTURE OF ROD A-2 AT 13-11/16 TO 14-9/32 IN. FROM BOTTOM OF FUEL COLUMN. Note that grain growth has occurred in the fuel center and mid radius regions.

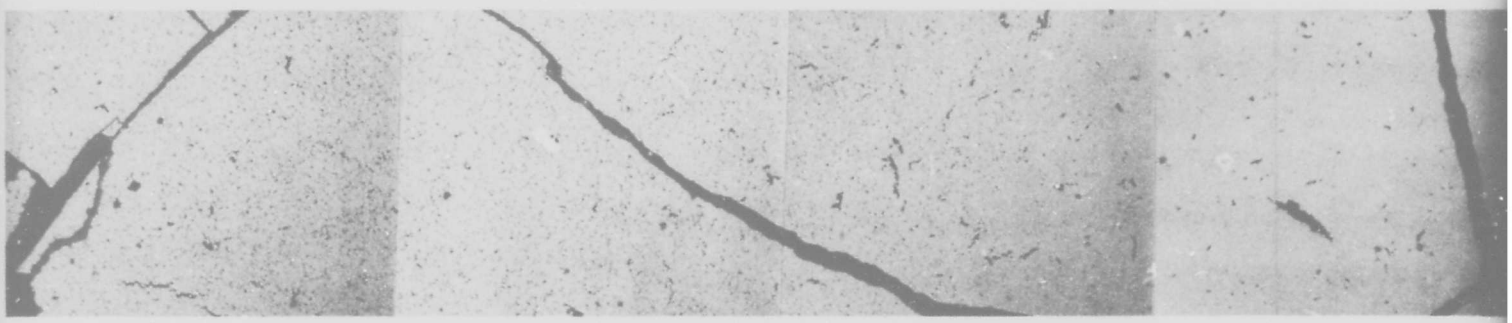

Original magnification 100X, reduced for reporting.
(a) As-Polished

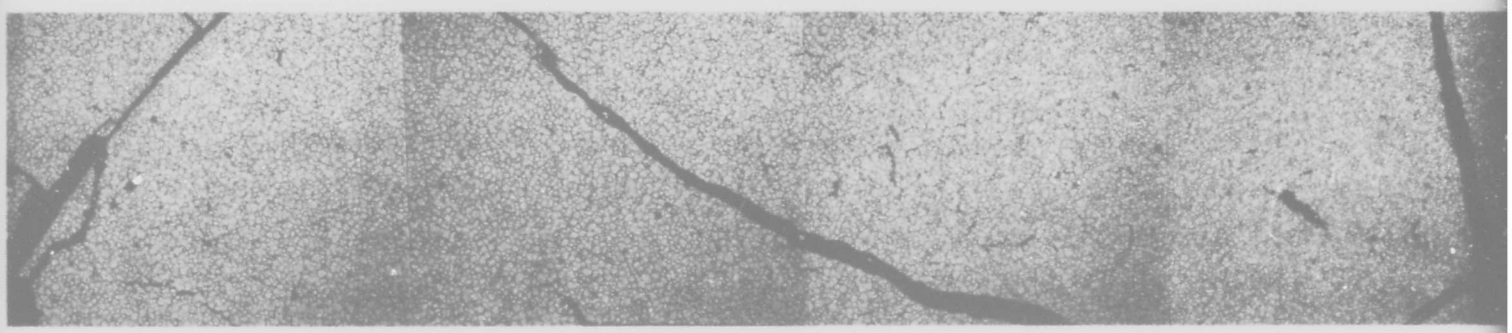

Original magnification 100X, reduced for reporting.
(b) Etched

FIGURE 22. LOW MAGNIFICATION RADIAL TRAVERSES OF METALLOGRAPHIC SAMPLE FROM ROD A
This illustrates the microstructural changes that have occurred in the

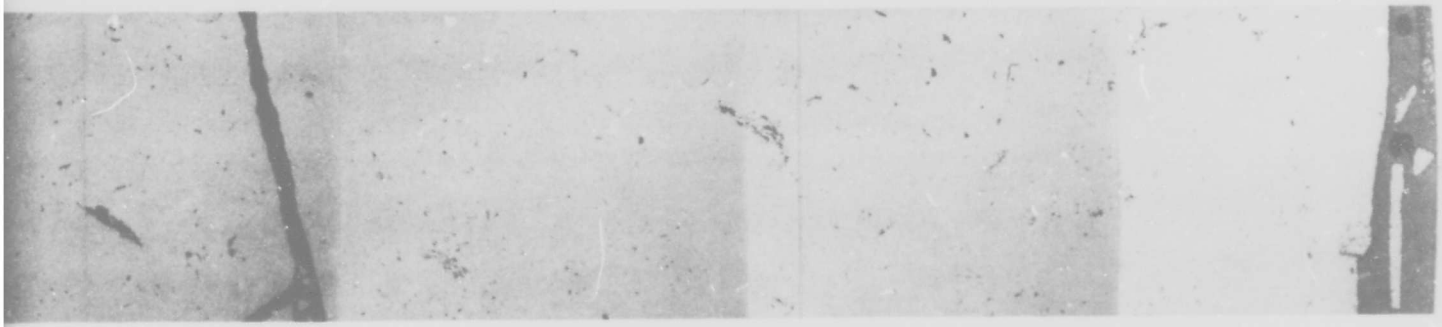

orting.

HC39647 - 39653

orting.

HC39720 - 39726

APHIC SAMPLE FROM ROD A-2 AT 13-11/16 - 14-9/32 IN. FROM BOTTOM OF FUEL COLUMN.
at have occurred in the high power region of Rod A-2.

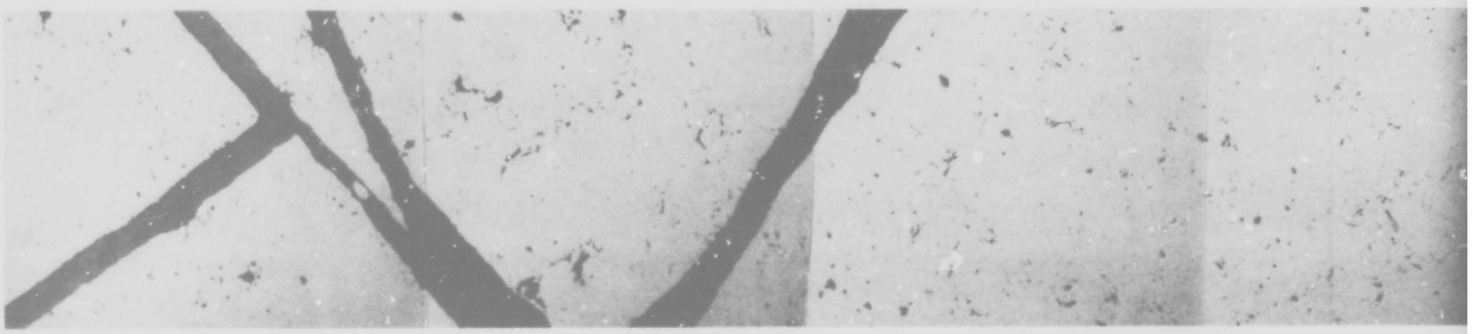

Original magnification 100X, reduced for reporting.

(a) As-Polished

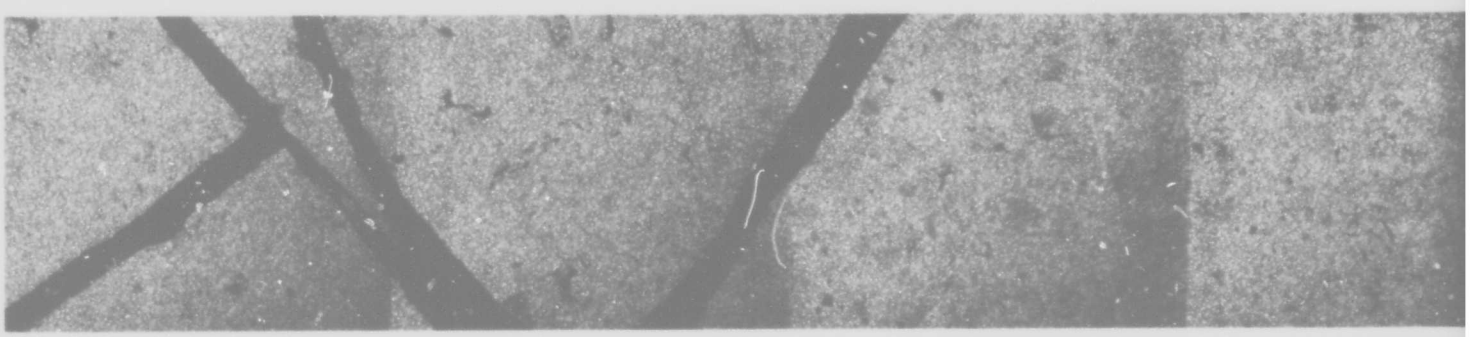

Original magnification 100X, reduced for reporting.

(b) Etched

FIGURE 23. LOW MAGNIFICATION IN RADIAL TRAVERSES OF METALLOGRAPHIC SAMPLE FROM RO
Note that the microstructure is uniform over the radius.

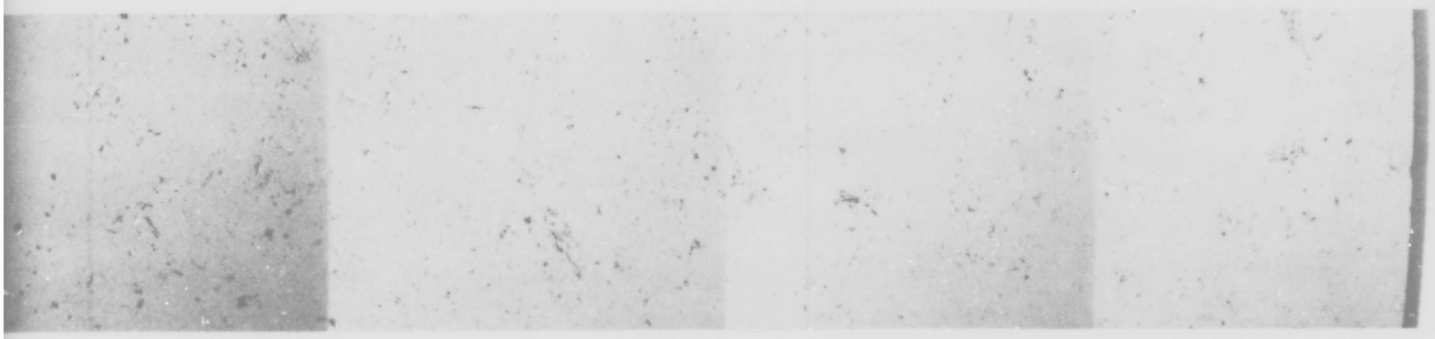

HC39627 - 39633

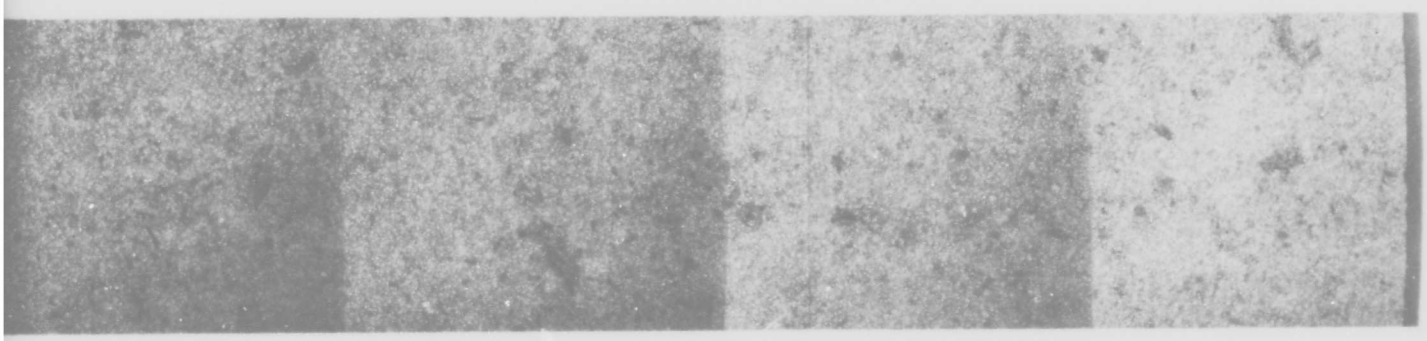

HC39690 - 39696

C SAMPLE FROM ROD F-8 AT 13-25/32 - 14-3/8 IN. FROM THE BOTTOM OF THE FUEL COLUMN.
s.

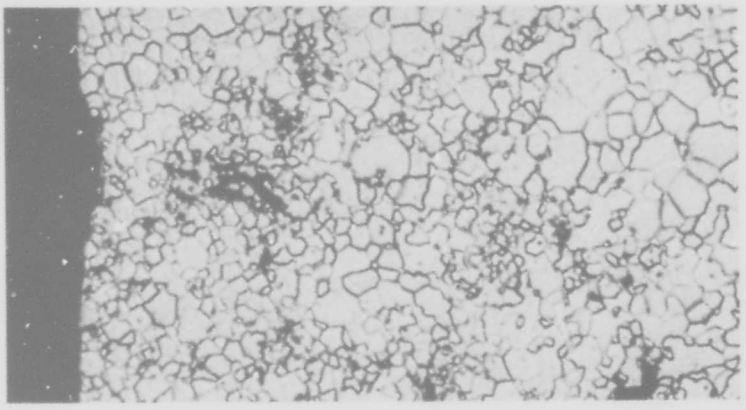

(a) Fuel Surface
500X
HC39697

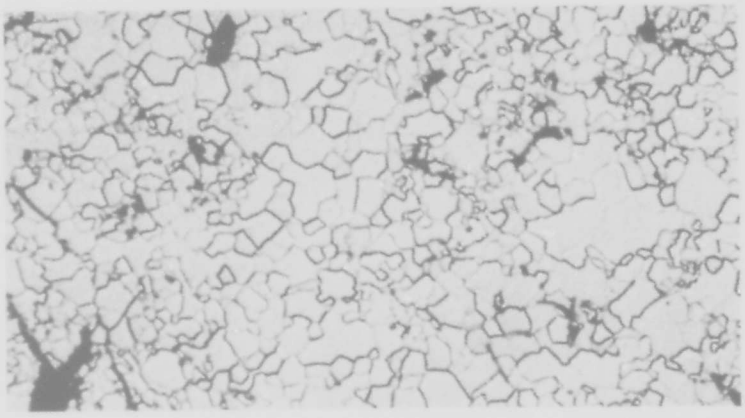

(b) Mid Radius
500X
HC39698

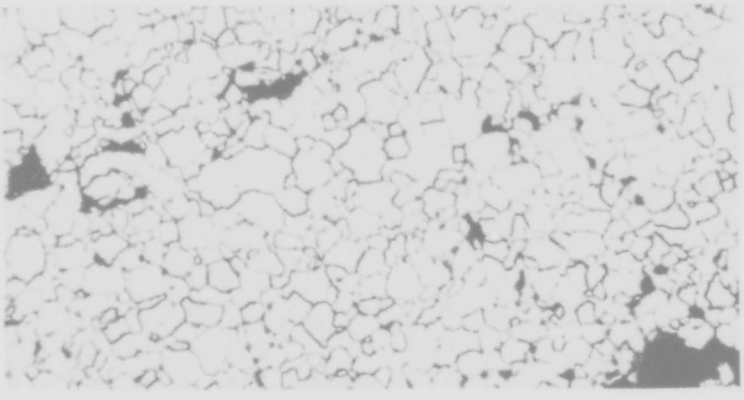

(c) Fuel Center
500X
HC39699

FIGURE 24. ETCHED MICROSTRUCTURE OF ROD F-8 AT 13-25/32 - 14-3/8 IN. Note that grain size is uniform in all radial positions. This is the second highest burnup metallographic specimen examined. Grain structure of lower burnup specimens were similar to this.

Summary and Conclusions

In-reactor fuel densification of the UO_2 fuel from the MH-1A Reactor was found to definitely have occurred. Because of uncertainties in the as-fabricated fuel density, the degree of densification could not be accurately determined. There were indications, however, that densification was complete after a burnup of about 8000 MWD/MTU. From that point, the fuel apparently started to swell slightly. Metallographic examination indicated that densification occurred by the annihilation of small as-fabricated pores.

On the basis of the sound appearance of the cladding, the fuel densification did not have any deleterious effect on the physical condition of the fuel rods or the fuel assembly. Absolutely no evidence of clad collapse was observed. Indeed, the loose fit of the fuel within the stainless steel cladding provided evidence that the cladding was strong enough to resist any creepdown even if fuel column gaps had existed during operation. Also, because of this loose fit, it is uncertain whether the fuel column gaps observed from gamma scanning and neutron radiography were present during operation. Fuel movement during transportation and handling could readily have produced the gaps.

However, the fuel densification may have implications in the analysis of a loss of coolant accident. It can be reasonably assumed that densification results in somewhat isotropic decreases in fuel pellet dimensions. Thus, as the fuel densifies, the fuel pellet diameter would decrease resulting in an increase in the fuel-clad gap width with an attendant decrease in the gap conductance. With isotropic pellet shrinkage, a 1.5 percent density increase represents a diametral decrease of about 2 mils in a MH-1A fuel pellet. Larger density increases would result in correspondingly larger diameter decreases.